Model Predictive Pulse Pattern Control with Very Fast Transient Responses

Tobias Geyer, *Senior Member, IEEE* and Nikolaos Oikonomou, *Member, IEEE*

***Abstract*—Closed-loop control and modulation of AC drives with offline computed optimized pulse patterns can be achieved by manipulating the time instants of the switching transitions. During torque steps, faults and low-voltage ride through operation, however, the transient response time is often rather slow, due to the absence of an appropriate voltage vector. By inserting additional switching transitions, deadbeat-like control can be achieved. The resulting control scheme combines the merits of optimized pulse patterns and deadbeat control, by providing very low current distortions at steady-state operation and very short response times during transients. Simulation results highlighting this are provided for a five-level inverter drive system.**

***Index Terms*—AC motor drives, medium-voltage drives, optimized pulse patterns, pulse width modulation, model predictive control, multilevel topologies.**

I. Introduction

Offline computed optimized pulse patterns (OPP) allow the minimization of the overall current distortion for a given switching frequency [2], [9]. In an AC drive setting, the current distortion is proportional to the harmonic losses in the stator winding of the electrical machine, while the switching frequency relates to the switching losses of the inverter. Traditionally, it has only been possible to use OPPs in a modulator driven by a slow control loop. This leads to very long transients and to harmonic excursions of the currents when the operating point is changed.

Generalizing the concept of trajectory tracking [5], [6], a model predictive control (MPC) method [10] has been recently proposed that achieves closed-loop control of an inverter driving an AC machine using OPPs [4]. This so-called model predictive pulse pattern controller (MP^{3}C) regulates the stator flux linkage vector of the machine along its optimal and pre-computed trajectory, by manipulating in real time the switching instants of the OPP's switching transitions. More specifically, the switching transitions are modified in time, such that the flux error is removed at a future time-instant. MP^{3}C addresses in a unified manner the tasks of the inner current control loop and modulator.

At steady-state operating conditions, due to the usage of OPPs, a nearly optimal ratio of harmonic current distortions per switching frequency is obtained [4]. Compared to state of the art trajectory controllers [6], MP^{3}C provides two advantages. First, a complicated observer structure to reconstruct the fundamental quantities is not required. Instead, the flux space vector, which is the controlled variable, can be estimated directly by sampling the currents and the dc-link voltage at regular sampling intervals. Second, by formulating an optimal control problem and using a receding horizon policy, the sensitivity to flux observer noise can be greatly reduced, as shown in [4].

During transients, such as load steps, large disturbances and faults, the electromagnetic torque is typically required to change in a step-like fashion or must follow a steep ramp. In an OPP, the switching transitions are not evenly distributed in time. Particularly at very low switching frequencies of a few hundred Hz, long time intervals might arise between two switching transitions. When a reference torque step is applied at the beginning of such an interval, a significant amount of time might elapse before the torque starts to change, resulting in a long initial time delay and often also in a prolonged settling time.

Once the controlled variable has started to change, the transient response might be sluggish and significantly slower than when using deadbeat control such as direct torque control (DTC) [11]. The sluggish response is typically due to the absence of a suitable voltage vector that moves the controlled flux vector with the maximum speed in the direction that ensures the fastest possible compensation of the flux error. In order to ensure a very fast response during transients, at least one phase needs to be switched to the upper or lower dc-link rail. In a low-voltage ride through setting, for example, this might imply reversing the voltage in at least one phase to its maximal or minimal value during most of the transient.

Directly related to the behavior of sluggish transient responses is the issue of current excursions during transients.

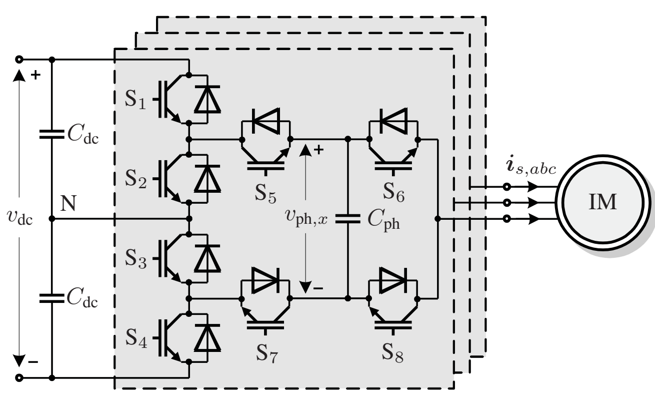

Fig. 1: Equivalent representation of the five-level active neutral point clamped (ANPC) voltage source inverter driving an induction machine

The authors are with ABB Corporate Research, Baden-Dättwil, Switzerland; e-mail: t.geyer@ieee.org, nikolaos.oikonomou@ch.abb.com

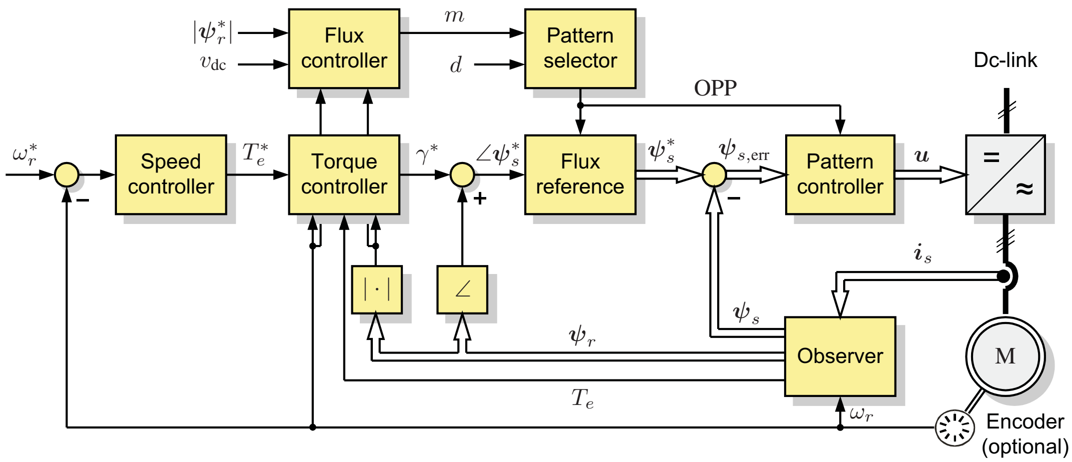

Fig. 2: Block diagram of the model predictive pulse pattern control (MP^{3}C) scheme

Such excursions might occur when the switching transitions, which are to be shifted in time so as to remove the flux error, are spread over a long time interval. This increase the risk that the flux vector is not moved along the shortest path from its current to its new desired position. Instead, the flux vector might temporarily deviate from this path, exceeding its nominal magnitude. This is equivalent to a large current, which might result in an over-current trip.

This paper proposes a solution to improve the performance of MP^{3}C during transients and (quasi) steady-state operation. When the flux error exceeds a given threshold, additional switching transitions are added to the OPP. As will be shown, with the insertion of additional switching transitions, the merits of OPPs and deadbeat control can be combined. Specifically, during transients, MP^{3}C achieves the very fast performance of a deadbeat controller, while during steady-state operation, the very low current distortions of OPPs are obtained.

The concept of introducing additional switching transitions has been previously mentioned in the literature in the context of trajectory tracking control, albeit only very briefly as a remark in [5], [6], [8]. This paper formally introduces the notion of inserting switching transitions and generalizes this concept by performing closed-loop rather than (open-loop) feedforward transition insertion.

II. Preliminaries

A. Drive System Case Study

To illustrate the proposed concepts, we will focus on a three-phase voltage source inverter with the total dc-link voltage v_{dc}. An active neutral point clamped (ANPC) inverter is considered that produces at each phase the five voltage levels $\{-\frac{v_{dc}}{2}, -\frac{v_{dc}}{4}, 0, \frac{v_{dc}}{4}, \frac{v_{dc}}{2}\}$. These voltages can be described by the integer variables $u_x \in \{-2, -1, 0, 1, 2\}$, with $x \in \{a, b, c\}$ denoting one of the three phases. The three-phase switch position is defined as $\boldsymbol{u}_{abc} = [u_a \; u_b \; u_c]^T$. To simplify the exposition, we will often drop the indices from $\boldsymbol{u}_{abc}$, simply writing $\boldsymbol{u}$.

As shown in Fig. 1, the three-phase inverter is connected to an induction machine with the stator flux vector $\boldsymbol{\psi}_{s,\alpha\beta} = [\psi_{s\alpha} \; \psi_{s\beta}]^T$, which is to be controlled by MP^{3}C. To simplify the notation, we will often drop the indices of the coordinate system from the flux vector, simply writing $\boldsymbol{\psi}_s$. The angular electrical stator and rotor frequencies of the machine are ω_s and ω_r, respectively. The ANPC topology is described in detail in [1], [7] and a state-space model was derived in [3].

B. Definitions

Throughout this paper, we will use normalized quantities. All variables $\boldsymbol{\xi}_{abc} = [\xi_a \; \xi_b \; \xi_c]^T$ in the three-phase abc system are transformed to $\boldsymbol{\xi}_{\alpha\beta} = [\xi_\alpha \; \xi_\beta]^T$ in the stationary and orthogonal $\alpha\beta$ coordinate system through the Clarke transformation $\boldsymbol{\xi}_{\alpha\beta} = \boldsymbol{P}\,\boldsymbol{\xi}_{abc}$ with

$$\boldsymbol{P} = \frac{2}{3}\begin{bmatrix} 1 & -\frac{1}{2} & -\frac{1}{2} \\ 0 & \frac{\sqrt{3}}{2} & -\frac{\sqrt{3}}{2} \end{bmatrix}, \quad \boldsymbol{P}^{-1} = \begin{bmatrix} 1 & 0 \\ -\frac{1}{2} & \frac{\sqrt{3}}{2} \\ -\frac{1}{2} & -\frac{\sqrt{3}}{2} \end{bmatrix}. \tag{1}$$

$\boldsymbol{P}^{-1}$ denotes the pseudo-inverse of $\boldsymbol{P}$.

We use $t_0 = kT_s$ to denote the current time-instant, where k is the current time-step and T_s is the sampling interval. Note that t_0 is real valued, while k is a natural number. Assume that the switch position in phase x changes at time t, i.e. $\Delta u_x(t) = u_x(t) - u_x(t - \mathrm{d}t)$ is nonzero, with $\mathrm{d}t$ being an infinitesimally small time step. We refer to $\Delta u_x(t)$ as a single-phase switching *transition*. Three-phase switching transitions are defined accordingly as $\boldsymbol{\Delta u}(t) = \boldsymbol{u}(t) - \boldsymbol{u}(t - \mathrm{d}t)$.

A *pulse* consists of two consecutive switching transitions in the same phase. The two switching transitions have opposite signs but do not necessarily have the same magnitude, as shown in the next section and in Fig. 5(b). In general, a pulse entails switching transitions in more than one phase.

III. MP^{3}C with Pulse Insertion

The proposed MP^{3}C scheme is shown in the block diagram in Fig. 2. It operates in the discrete time domain and is

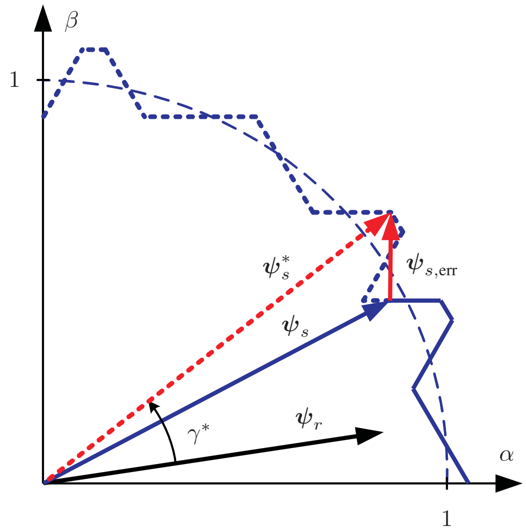

Fig. 3: Stator flux vector $\boldsymbol{\psi}_s$, rotor flux vector $\boldsymbol{\psi}_r$, reference flux vector $\boldsymbol{\psi}_s^*$ and stator flux error $\boldsymbol{\psi}_{s,\text{err}}$ in stationary coordinates

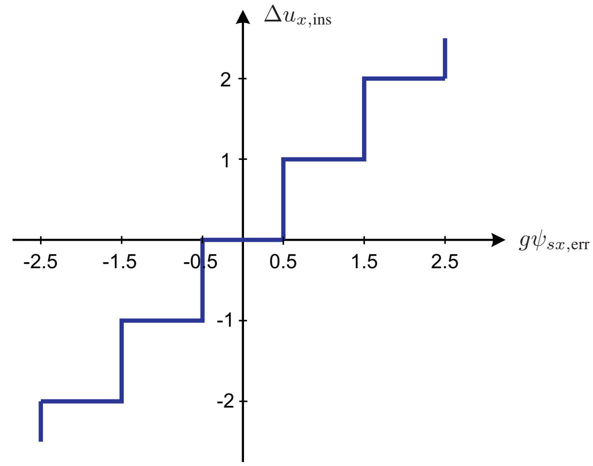

Fig. 4: Definition of the per-phase error bands on the stator flux error in phase x, with $x \in \{a, b, c\}$. The switching transition to be inserted is denoted by $\Delta u_{x,\text{ins}}$

activated at equally spaced time-instants $t_0 = kT_s$. The control problem is formulated and solved in stationary orthogonal coordinates. The algorithm comprises the following six steps, which are executed at the time-instant t_0. Compared to the standard MP^{3}C algorithm proposed in [4], Step 3 is augmented by an additional unit that inserts additional switching transitions when required.

Step 1. Estimate the stator and rotor flux vectors in the stationary reference frame. This yields $\boldsymbol{\psi}_s = [\psi_{s\alpha}\ \psi_{s\beta}]^T$ and $\boldsymbol{\psi}_r = [\psi_{r\alpha}\ \psi_{r\beta}]^T$. Let $\angle\boldsymbol{\psi}$ denote the angular position of a flux vector and $|\boldsymbol{\psi}|$ its magnitude.

Compensate for the delay introduced by the controller computation time by rotating the estimated stator and rotor flux vectors by $\omega_s T_s$ forward in time, i.e. $\angle\boldsymbol{\psi}_s = \angle\boldsymbol{\psi}_s + \omega_s T_s$ and accordingly for the rotor flux.

Step 2. Compute the reference of the stator flux vector $\boldsymbol{\psi}_s^*$. Recall that the electromagnetic torque T_e produced by the machine can be written as $T_e = k_r |\boldsymbol{\psi}_s|\,|\boldsymbol{\psi}_r| \sin(\gamma)$, where k_r is the rotor coupling factor, and γ is the angle between the stator and the rotor flux vectors. Therefore, the desired angle between the stator and rotor flux vectors is

$$\gamma^* = \sin^{-1}\left(\frac{T_e^*}{k_r |\boldsymbol{\psi}_s|\,|\boldsymbol{\psi}_r|}\right). \tag{2}$$

The reference flux vector is then obtained by integrating the nominal three-phase pulse pattern along the time axis; the reference angle $\angle\boldsymbol{\psi}_r + \gamma^*$ constitutes the upper limit of the integral. The resulting instantaneous reference flux vector has, in general, a magnitude and angle that slightly differ from their respective values on the unitary circle, see Fig. 3. The vector diagram in this figure provides a graphical summary of the derivation of the reference flux vector.

Step 3.1. Compute the stator flux error, which is the difference between the reference and the estimated stator flux vector according to

$$\boldsymbol{\psi}_{s,\text{err}} = \boldsymbol{\psi}_s^* - \boldsymbol{\psi}_s\,, \tag{3}$$

see also Fig. 3. Map the stator flux error from the orthogonal $\alpha\beta$ coordinate system into the three-phase abc system

$$\boldsymbol{\psi}_{s,abc,\text{err}} = \boldsymbol{P}^{-1}\,\boldsymbol{\psi}_{s,\text{err}}\,. \tag{4}$$

Step 3.2. In each phase, introduce error bands on the stator flux error, as shown in Fig. 4. Based on those, determine whether an incremental switching vector, the three-phase switching transition $\Delta\boldsymbol{u}_{\text{ins}}$, is to be inserted. If this is the case, determine for each phase the magnitude and sign of the switching transition. These two statements can be expressed in a compact way as

$$\Delta\boldsymbol{u}_{\text{ins}} = \text{round}(g\boldsymbol{\psi}_{s,abc,\text{err}})\,, \tag{5}$$

where the gain g is a user-defined scalar parameter. Note that the gain and rounding operation implicitly define the error bands[1].

As shown in Fig. 4, the magnitude and sign of the flux error in abc determines the magnitude and sign of the additional switching transition $\Delta\boldsymbol{u}_{\text{ins}}$. This is done for each phase separately. If the switching transition is zero in all three phases, i.e. when $|g\psi_{sx,\text{err}}| < 0.5$, with $x \in \{a, b, c\}$, then no additional switching transition is inserted. When the flux error is positive, which is caused by too small a stator flux, additional volt-second is to be added, which is equivalent to adding a positive switching transition and hence a positive pulse[2].

[1]Since the stator flux is the integral of the inverter switch positions weighted with half the dc-link voltage, i.e. $\boldsymbol{\psi}_{s,abc}(t) = \boldsymbol{\psi}_{s,abc}(0) + 0.5v_{\text{dc}}\int_0^t \boldsymbol{u}_{abc}(\tau)d\tau$, the term $0.5v_{\text{dc}}$ is implicitly included in the gain g.

[2]Specifically, an additional switching transition of magnitude one is required in phase x, $\Delta u_{x,\text{ins}} = 1$, if $0.5 \leq g\psi_{sx,\text{err}} < 1.5$. Correspondingly, a transition of magnitude $\Delta u_{x,\text{ins}} = 2$ is added in case $1.5 \leq g\psi_{sx,\text{err}} < 2.5$, and so on. Negative switching transitions are added in the presence of negative flux errors.

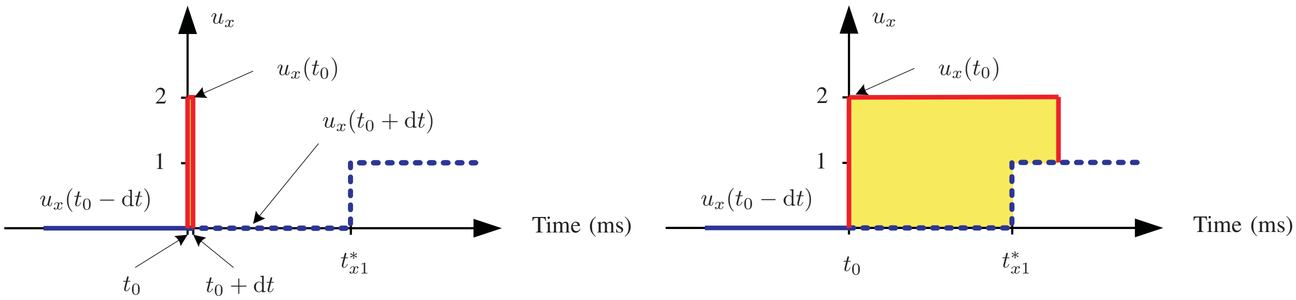

(a) Insertion of an additional pulse to the nominal OPP. The width of the pulse is arbitrarily close to zero

(b) Modification of the additional pulse by MP^{3}C to generate the required volt-seconds

Fig. 5: Insertion of a pulse of amplitude two and width $\mathrm{d}t$ at the current time-instant t_0 and modification by the pattern controller to achieve fast closed-loop control

Step 3.3. Ensure that short pulses are not added repeatedly, giving rise to a chattering phenomenon and an increase in the switching frequency. This issue can be avoided by ensuring that, when switching transitions are inserted, the magnitude of the inserted transitions decreases in each phase while maintaining its sign. Specifically, for each phase, the required additional transition is modified when required, according to the following three rules.

1) If $||\Delta \boldsymbol{u}_{\text{ins}}(k-1)|| > 0$ and $\Delta u_{x,\text{ins}}(k-1) = 0$ then $\Delta u_{x,\text{ins}}(k) = 0$.
2) If $\Delta u_{x,\text{ins}}(k-1) > 0$ then $\Delta u_{x,\text{ins}}(k) = \min(\max(\Delta u_{x,\text{ins}}(k), 0), \Delta u_{x,\text{ins}}(k-1))$.
3) If $\Delta u_{x,\text{ins}}(k-1) < 0$ then $\Delta u_{x,\text{ins}}(k) = \max(\min(\Delta u_{x,\text{ins}}(k), 0), \Delta u_{x,\text{ins}}(k-1))$.

The first rule ensures that when a pulse insertion campaign has ended in phase x but is still ongoing in another phase, it is not to be restarted in phase x, before it has ended in all three phases. The second and third rules impose that the magnitudes of the inserted switching transitions decrease monotonically until they reach zero.

Step 3.4. Add the additional switching transition $\Delta \boldsymbol{u}_{\text{ins}}$ to the nominal pulse pattern (with the nominal switch positions and the nominal transition times). This process is visualized in Fig. 5(a) and entails the following three steps.

1) Read out the nominal OPP from the look-up table. Build the nominal switching sequence starting at time-instant t_0 sufficiently far into the future. In Fig. 5(a), the nominal switching sequence in phase x is shown as the dotted (blue) line.
2) Determine the value of the switch position at time t_0, which is given by $\boldsymbol{u}(t_0) = \boldsymbol{u}(t_0 - \mathrm{d}t) + \Delta \boldsymbol{u}_{\text{ins}}(t_0)$. In here, the switch position currently applied to the inverter is denoted by $\boldsymbol{u}(t_0 - \mathrm{d}t)$. In case $\boldsymbol{u}(t_0)$ exceeds the set of available switch positions of the inverter, $\boldsymbol{u}(t_0)$ is saturated at the maximal or minimal attainable switch position[3].
3) Add a pulse of the infinitesimally small width $\mathrm{d}t$, by adding a switching transition at time t_0 from $\boldsymbol{u}(t_0 - \mathrm{d}t)$ to $\boldsymbol{u}(t_0)$ and another switching transition with opposite sign at time $t_0 + \mathrm{d}t$ from $\boldsymbol{u}(t_0)$ to $\boldsymbol{u}(t_0 + \mathrm{d}t)$[4]. The pulse starts at time-instant t_0 and ends at $t_0 + \mathrm{d}t$. The volt-second of the inserted pulse is zero. The added pulse is shown as a straight (red) line in Fig. 5(a). The resulting switching sequence consists of the nominal switching transitions of the OPP and an additional pulse at time t_0 of width $\mathrm{d}t$.

Step 4. In the fourth step, the pulse pattern controller is executed, by formulating and solving a quadratic program (QP). The quadratic objective function penalizes the uncorrected flux error (the controlled variable) and the modifications to the switching instants (the manipulated variable) subject to linear constraints on the switching instants. The modified switching instants are aggregated in the vector

$$\Delta \boldsymbol{t} = [\Delta t_{a1} \; \Delta t_{a2} \ldots \Delta t_{an_a} \; \Delta t_{b1} \ldots \Delta t_{bn_b} \; \Delta t_{c1} \ldots \Delta t_{cn_c}]^T . \tag{6}$$

For phase a, for example, the correction of the i-th transition time is given by $\Delta t_{ai} = t_{ai} - t^*_{ai}$, where t^*_{ai} denotes the nominal switching instant of the i-th transition Δu_{ai}. Moreover, n_a denotes the number of switching transitions in phase a that are within the prediction horizon. The quantities for phases b and c are defined accordingly.

Starting at time t_0, the pattern controller modifies the switching instants of the three-phase switching sequence, which, in general, includes additional pulses. The switching

[3]This implies that it might not be possible to implement the inserted switching transition to the full extent requested. As an example, consider a five-level inverter. Assume that the currently applied switch position in phase x is $u_x(t_0 - \mathrm{d}t) = 1$ and that the additional switching transition $\Delta u_x(t_0) = 3$ has been requested. It is only possible to implement the switch position $u_x(t_0) = 2$, which corresponds to an inserted transition of $\Delta u_x(t_0) = 1$ in phase x.

[4]Special care needs to be taken to ensure that the magnitude of the second switching transitions (at time $t_0 + \mathrm{d}t$) is correct, since the first and second switching transitions do not necessarily sum up to zero. This case arises, for example, when a nominal switching transition is scheduled at t_0. The switch position $\boldsymbol{u}(t_0 + \mathrm{d}t)$ must match the nominal switch position at time $t_0 + \mathrm{d}t$.

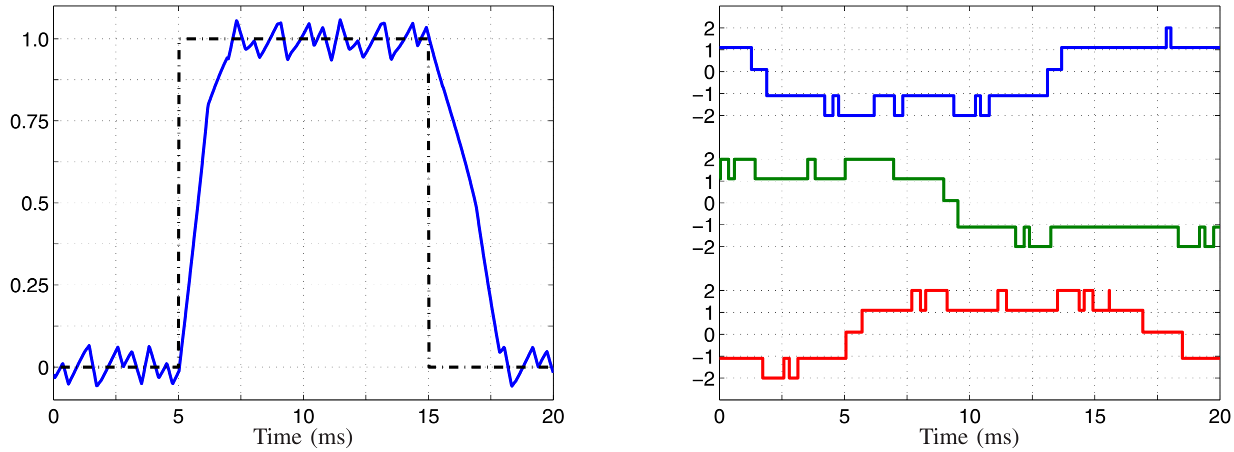

(a) Electromagnetic torque T_e and its reference

(b) Three-phase switch position $\boldsymbol{u}$

Fig. 6: Standard deadbeat MP^{3}C: closed-loop response to step changes in the torque reference

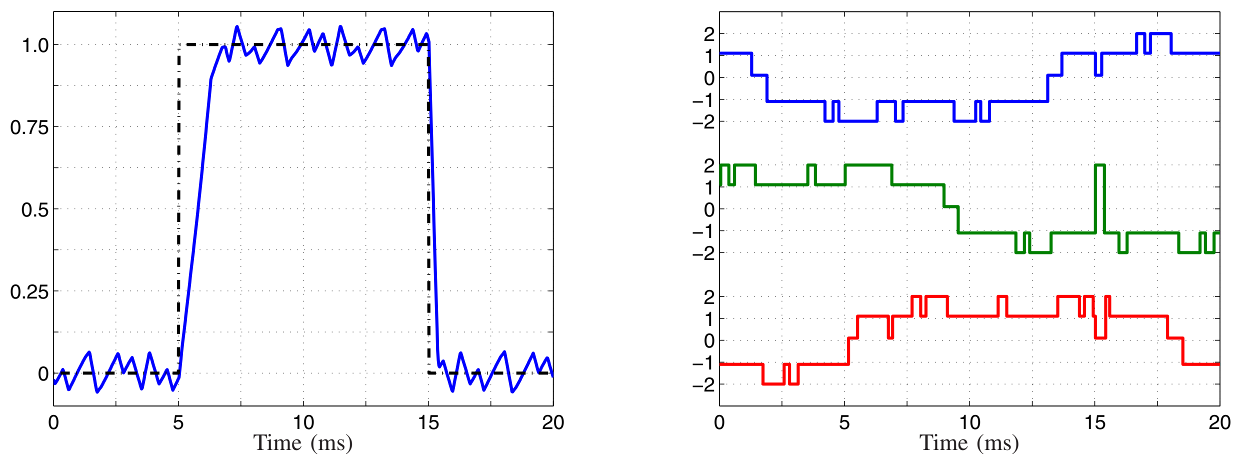

(a) Electromagnetic torque T_e and its reference

(b) Three-phase switch position $\boldsymbol{u}$

Fig. 7: Fast deadbeat MP^{3}C with pulse insertion: closed-loop response to step changes in the torque reference

instants are manipulated such that the required volt-second correction is generated that removes the flux error and drives the stator flux vector back to its reference trajectory as quickly as possible.

An alternative MP^{3}C formulation is based on a deadbeat controller, which considers switching transitions in at least two phases. This variation is computationally simpler, faster during transients, but also more sensitive to flux observer noise. For more details on formulating and solving the MP^{3}C problem, the reader is referred to [4].

Step 5. Remove switching transitions that will occur within the sampling interval. This can be accomplished by updating a pointer to the look-up table that stores the switching angles of the OPP and the respective three-phase switch positions.

Step 6. Derive the switching commands over the sampling interval, i.e. the switching instants and the associated switch positions. The switching commands are sent to the gate units of the semiconductor switches in the inverter.

IV. Performance Evaluation

Simulation results during torque steps are provided in this section, which compare the performance of MP^{3}C with pulse insertion with the one of standard MP^{3}C, highlighting the merits of the proposed method.

Consider again the five-level ANPC inverter shown in Fig. 1. The inverter is connected to a 50 Hz medium-voltage induction machine with a leakage inductance of $L_\sigma = 0.18$ per unit (pu). An in-depth description of the drive system, as well as the detailed machine and inverter parameters, are provided in [3]. The simulations were run at $\omega_s = 0.8$ pu using an OPP with pulse number $d = 6$. Torque steps from $T_e = 0$ to 1 pu

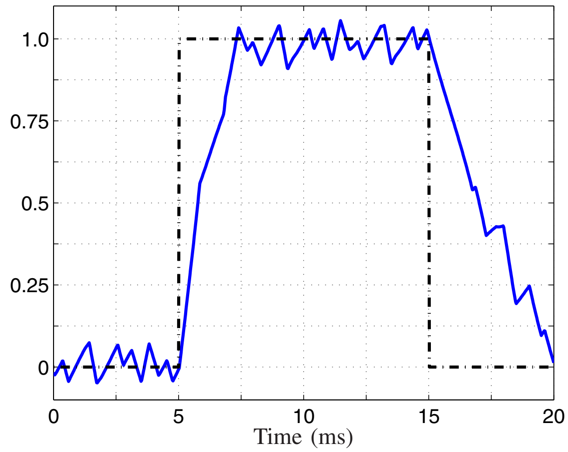

(a) Standard QP MP^{3}C

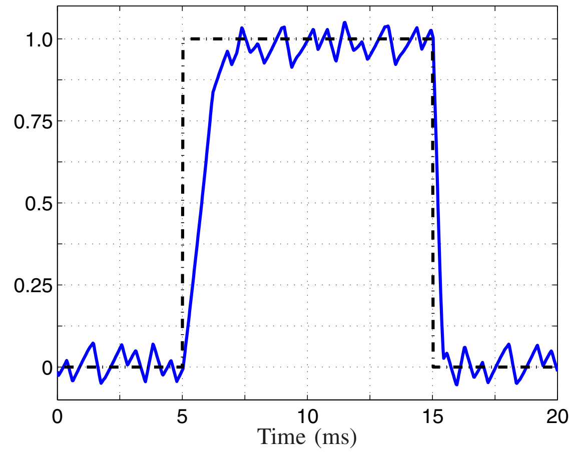

(b) Fast QP MP^{3}C with pulse insertion

Fig. 8: Closed-loop response of QP MP^{3}C to step changes in the torque reference. The standard QP approach is compared with the fast QP method with pulse insertion

and back were applied at time-instants $t = 5$ and $t = 15$ ms, respectively. In (5), the gain was set to $g = 20$.

Fig. 6 shows the torque response and the sequence of switch positions for standard deadbeat MP^{3}C without pulse insertion capability. For pulse insertion, the corresponding results are shown in Fig. 7. With the machine operating close to its nominal speed, the available voltage margin is small. As a result, pulse insertion provides only a minor benefit during positive torque steps, when a large positive voltage vector is required to quickly move the stator flux forward.

During negative torque steps at close to nominal speed, however, inserting pulses significantly reduces the torque settling time—in this case from about 5 ms to less than 1 ms, as shown in Fig. 7. MP^{3}C with pulse insertion generates a large negative voltage vector, thus temporarily inverting the voltage applied to the machine. Specifically, a large positive pulse in the voltage of phase b is inserted, by inverting the sign of the phase b voltage at $t = 15$ ms, and switching from $u_b = -1$ to $u_b = 2$. This large voltage step is necessary to drive the electromagnetic torque to zero as quickly as possible. This drastic speed-up of the torque response is at the expense of a temporary increase in the switching effort, due to the insertion of additional pulses in the three phases.

In a practical converter setting, large voltage steps might neither be desirable nor feasible. Restrictions are usually imposed in order to limit the rate of change of the voltage, i.e. the dv/dt. This is due to the fact that high dv/dt values are detrimental to the lifetime of the machine windings in an electrical drive setting. Apart from that, switching by more than one step up or down per phase might be prohibited by switching restrictions in the inverter, which are induced by the topology used. When such limitations apply, the switch positions commanded by MP^{3}C are not necessarily applied to the inverter. The large positive pulse in phase b in Fig. 7, for example, is then slightly modified. Since the width of the pulse is about 1 ms and switching restrictions are in the range of several tens of μs, the impact of these modifications on MP^{3}C and the torque transient are minor. In particular, the closed-loop characteristic of MP^{3}C is well suited to handle these mismatches.

When using QP MP^{3}C the performance improvement is even more significant, as can be seen in Fig. 8. For the QP method, a fixed prediction horizon of 20° was used. The use of QP over deadbeat MP^{3}C is in general preferred due to the superior robustness properties of the QP MP^{3}C method. Specifically, as the prediction horizon in MP^{3}C is extended, the sensitivity of MP^{3}C to flux estimation noise is reduced and, as a result, the current THD is improved. For a detailed robustness analysis of MP^{3}C, the reader is referred to [4]. The robustness of QP MP^{3}C is not affected by the insertion of pulses.

V. Discussion and Conclusion

The proposed pulse insertion concept provides the controller, when required, with an additional degree of freedom to remove the flux error as quickly as possible. Switching transitions can be inserted and switching patterns synthesized that correspond to voltage vectors with magnitudes and angles that differ greatly from the voltage vectors inherent to the nominal OPP. Specifically, the phase voltage applied to the stator windings of the machine can be temporarily increased to its maximum value and/or its sign can be inverted.

The inserted pulses correspond to effectively zero volt-second, thus resembling a virtual pulse. The second switching transition leading back to the nominal switching sequence is not determined when the first switching transition is inserted. Instead, the time-instant of the second transition is adjusted and controlled in a closed-loop fashion by MP^{3}C, following the receding horizon policy of MPC [10]. Specifically, the width of the pulse and the amount of volt-second generated by it is adjusted, while the inserted pulse is being applied. At subsequent sampling instants, the pulse width is readjusted to account for flux observer noise, disturbances affecting the stator flux, further changes in the torque reference and restrictions on the allowed dv/dt.

As a consequence, the step size of the second transition is not determined at the time the pulse is inserted. As can be seen in Fig. 5(b), when shifting the second transition of the pulse beyond the nominal switching instant of the next transition t_{x1}^{*}, the step size is reduced from -2 to -1.

The closed-loop control paradigm of the proposed pulse insertion method is in stark contrast to the method previously mentioned in the literature [5], [6], [8]. The latter appears to rely on an *open-loop* pulse insertion paradigm, using a feedforward approach, in which both switching transitions are determined at the time they are inserted. Apart from that, depending on the flux error and the error bounds, in the proposed method switching transitions are inserted in one, two or three phases, rather than always in two phases, as previously.

REFERENCES

[1] P. Barbosa, P. Steimer, J. Steinke, L. Meysenc, M. Winkelnkemper, and N. Celanovic. Active neutral-point-clamped multilevel converters. In *Proc. IEEE Power Electron. Spec. Conf.*, pages 2296–2301, Recife, Brasil, Jun. 2005.

[2] G. S. Buja. Optimum output waveforms in PWM inverters. *IEEE Trans. Ind. Appl.*, 16(6):830–836, Nov./Dec. 1980.

[3] T. Geyer and S. Mastellone. Model predictive direct torque control of a five-level ANPC converter drive system. *IEEE Trans. Ind. Appl.*, 48(5):1565–1575, Sep./Oct. 2012.

[4] T. Geyer, N. Oikonomou, G. Papafotiou, and F. Kieferndorf. Model predictive pulse pattern control. *IEEE Trans. Ind. Appl.*, 48(2):663–676, Mar./Apr. 2012.

[5] J. Holtz and B. Beyer. Off-line optimized synchronous pulsewidth modulation with on-line control during transients. *EPE Journal*, 1(3):193–200, Dec. 1991.

[6] J. Holtz and N. Oikonomou. Synchronous optimal pulsewidth modulation and stator flux trajectory control for medium-voltage drives. *IEEE Trans. Ind. Appl.*, 43(2):600–608, Mar./Apr. 2007.

[7] F. Kieferndorf, M. Basler, L.A. Serpa, J.-H. Fabian, A. Coccia, and G. Scheuer. A new medium voltage drive system based on ANPC-5L technology. In *Proc. IEEE Int. Conf. Ind. Technol.*, pages 605–611, Viña del Mar, Chile, Mar. 2010.

[8] N. Oikonomou. *Control of medium-voltage drives at very low switching frequency*. PhD thesis, University of Wuppertal, 2008.

[9] H. S. Patel and R. G. Hoft. Generalized techniques of harmonic elimination and voltage control in thyristor inverters: Part I–Harmonic elimination. *IEEE Trans. Ind. Appl.*, 9(3):310–317, May/Jun. 1973.

[10] J. B. Rawlings and D. Q. Mayne. *Model predictive control: Theory and design*. Nob Hill Publ., Madison, WI, USA, 2009.

[11] I. Takahashi and T. Noguchi. A new quick response and high efficiency control strategy for the induction motor. *IEEE Trans. Ind. Appl.*, 22(2):820–827, Sep./Oct. 1986.